

Theoretical analysis of the thermal conductivity of $\text{YBa}_2\text{Cu}_3\text{O}_{7-\delta}$ single crystals

S. D. Peacor, R. A. Richardson, F. Nori, and C. Uher

Department of Physics, University of Michigan, Ann Arbor, Michigan 48109

(Received 30 May 1991)

We analyze the in-plane thermal conductivity of single-crystal $\text{YBa}_2\text{Cu}_3\text{O}_{7-\delta}$. Our theoretical fit provides an excellent description of the experimental data throughout the temperature range $10 \text{ K} < T < 200 \text{ K}$. From this fit, we can extract information about the lattice microstructure and the electronic contribution to the total thermal conductivity. Our calculations indicate that long-wavelength phonons, with mean free paths of the order of the crystal thickness, contribute significantly to the thermal conductivity up to $\sim 75 \text{ K}$. The phonon-electron coupling strength λ for the phonons which dominate in the heat-conduction process is calculated to lie in the range $0.03 < \lambda < 0.08$. In addition, we extract a value of $(1.6 \pm 0.3)\Delta_{\text{BCS}}$ for the superconducting energy gap.

I. INTRODUCTION

The thermodynamic and transport properties of Cu-O high- T_c superconductors have been extensively investigated in the past few years. The thermal conductivity κ is among a small group of transport measurements that provide a nonvanishing signal even below the superconducting transition temperature T_c . Heat conduction¹ in Cu-O plane superconductors is typified by a dramatic increase in the thermal conductivity as the temperature is lowered below T_c . Initial measurements on sintered samples indicated a peak in κ near $T_c/2$, with a value approximately 20% higher than the value at T_c . More recently, this increase has been shown to approach 100% in single crystals.^{2,3} Interestingly, the characteristic peak in κ is seen only when the temperature gradient is applied parallel to the ab plane. As of yet, no observable change near T_c has been detected when the heat flow is parallel to the c axis.⁴⁻⁶ Tewordt and Wölkhausen⁷ have presented a model that attempts to describe the thermal conductivity of Cu-O superconductors in the context of the BCS theory. Using this model they fit, with moderate success, thermal conductivity data from sintered samples. Florentiev *et al.*³ applied a similar model to their single-crystal thermal conductivity data and found good agreement between theory and experiment for $T < T_c$. In a later publication, Tewordt and Wölkhausen⁸ extended their model to include the possibilities of strong coupling and d -wave pairing, and considered the effect of the structural anisotropy on κ .

In this paper we present a detailed analysis of the

thermal conductivity of single crystals of $\text{YBa}_2\text{Cu}_3\text{O}_{7-\delta}$ measured recently.² From a theoretical fit, we derive useful information about the lattice and electronic transport parameters. The lattice thermal conductivity dominates the total thermal conductivity, and we illustrate graphically the relative contribution to the lattice thermal resistance by the different phonon scattering centers, e.g., crystal boundaries, lattice defects, electrons, and other phonons (Umklapp processes). Variations in the theoretical coefficients from sample to sample are shown to correspond to qualitative differences in the crystal microstructure. Perhaps surprisingly, we find that long-wavelength phonons, with $\Lambda \sim 100 \text{ \AA}$ at 77 K , dominate the heat transfer process. Using the expression derived in Ref. 7, the electron-phonon coupling strength of the phonons responsible for the heat conduction is found to be much smaller than previously reported for Cu-O superconductors, and we indicate reasons for this discrepancy. In addition, we suggest that the thermal conductivity is enhanced by superconducting fluctuations near T_c . Finally, we extract a value for the superconducting energy gap.

II. THEORETICAL MODEL

The total thermal conductivity of a superconductor is the sum of an electronic contribution κ_e and a lattice contribution κ_p :

$$\kappa = \kappa_e + \kappa_p . \tag{1}$$

The lattice contribution is expressed by the equation⁷⁻¹⁰

$$\kappa_p(T) = \frac{k_B}{2\pi^2v} \left[\frac{k_B}{\hbar} \right]^3 T^3 \int_0^{\Theta_D/T} dx \frac{x^4 e^x}{(e^x - 1)^2} \int_0^1 d\xi \frac{3}{2} (1 - \xi^2) \tau(T, x, \xi) , \tag{2}$$

where

$$\tau^{-1}(T, x, \xi) = B + D_p T^4 x^4 + D_{sf} T^2 x^2 + ETxg(x, y)(1 - \xi^2)^{3/2} + UT^4 x^2 . \tag{3}$$

Here $\tau^{-1}(T, x, \zeta)$ is the total phonon relaxation rate, Θ_D is the Debye temperature, v is the phonon velocity, x is the reduced phonon energy $\hbar\omega/k_B T$, and y is the reduced superconducting energy gap $\Delta(t)/k_B T$, where $t = T/T_c$. The coefficients B , D_p , D_{sf} , E , and U describe the magnitude of the phonon scattering by boundaries, point defects, sheetlike faults, electrons, and other phonons (Umklapp scattering), respectively. We have employed the calculation by Tewordt and Wölkhausen⁸ in which they take into account the anisotropy of the Cu-O superconductors in deriving κ . The integration over ζ , where $\zeta = \cos\theta$ is the polar angle with respect to the c axis, incorporates the anisotropy of the phonon-electron interaction and momentum conservation in the ab plane. As described in Ref. 7, the coefficient E (related to the coefficient γ of Ref. 7) is directly proportional to the phonon-electron coupling constant, and the function $g(x, y)$ contains the information regarding the superconductivity of the sample.

More specifically, $g(x, y)$ is equal to the ratio of the phonon-electron scattering times in the normal and superconducting states, τ_{pe}^n/τ_{pe}^s . It is the dramatic decrease in τ_{pe}^n/τ_{pe}^s that leads to the marked increase in the thermal conductivity of high- T_c superconductors as the temperature is lowered below T_c . This ratio has been derived by Bardeen, Rickayzen, and Tewordt⁹ for BCS-type s -wave pairing and more recently by Tewordt and

TABLE I. Coefficients of Eqs. (2), (3), and (4) used to fit samples 1, 1A, and 2 as shown in Fig. 1.

Sample	1	1A	2
K ($\text{W m}^{-1}\text{K}^{-1}$)	4.4	4.4	1.5
B (sec^{-1})	5.0×10^7	5.0×10^7	3.4×10^7
D_p ($\text{K}^{-4}\text{sec}^{-1}$)	370	370	723
D_{sf} ($\text{K}^{-2}\text{sec}^{-1}$)	1.7×10^5	3.2×10^5	2.2×10^5
E ($\text{K}^{-1}\text{sec}^{-1}$)	1.8×10^8	1.8×10^8	6.4×10^7
χ	1.74	1.74	1.44
U ($\text{K}^{-4}\text{sec}^{-1}$)	82	82	53

Wölkhausen⁸ for the d -wave pairing case. The latter authors suggest that thermal conductivity data can be more closely fit with the d -wave model. We find, however, that the s -wave model provides an excellent description of our data and is the form that will be used throughout this discussion. As in Ref. 7, we employ a scaled superconducting energy gap, $\Delta(t) = \chi\Delta_{\text{BCS}}(t)$, where χ is a constant.

We can gain insight into the form of the electronic contribution to the thermal conductivity by examining the electrical resistivity ρ . In high- T_c superconductors, ρ in the normal state is a nearly linear function of T . Thus, by invoking the Wiedemann-Franz law, we can approximate the temperature dependence of the electronic thermal conductivity to be a constant above the superconducting transition temperature. Below T_c , however, the charge carriers condense into Cooper pairs, which do not transfer heat. The temperature dependence of κ_e for $T < T_c$ is very different depending on whether the electrons are scattered predominantly by defects or predominantly by phonons.¹¹ We cannot fit our data if we assume the former case (Eq. 1.5 of Ref. 11), which yields a more gradual decrease in κ_e below T_c than the latter scenario. We adopt, then, the description where phonons are the dominant electron scatterers. This case has been investigated in detail by Tewordt¹² and Geilikman, Dushenat, and Chechetkin,¹³ and they derive expressions for the dependence of κ_e on T , which are very similar to one another. In our study we have employed the results of Geilikman, Dushenat, and Chechetkin¹³ in which they have tabulated $\kappa_{ep}^s/\kappa_{ep}^n$, the ratio of the electronic thermal conductivity in the superconducting state and normal states, as a function of the reduced temperature. As with the lattice contribution to κ , we employ a scaled energy gap, where $\Delta(t) = \chi\Delta_{\text{BCS}}(t)$. The electronic contribution is then estimated as

$$\kappa_e = \begin{cases} K, & T > T_c \\ K \frac{\kappa_{ep}^s}{\kappa_{ep}^n}, & T < T_c, \end{cases} \quad (4)$$

where K is a constant.

We combine Eqs. (1)–(4) in order to fit the data, and we find excellent agreement between the theoretical curve and experiment. The results are illustrated in Fig. 1, and the respective fitting coefficients are listed in Table I.

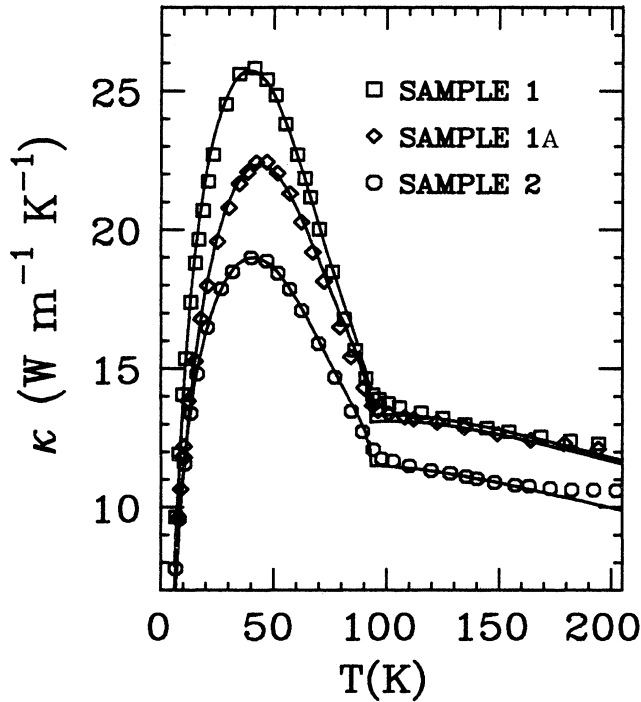


FIG. 1. Experimental data and theoretical curves showing the thermal conductivity of three $\text{YBa}_2\text{Cu}_3\text{O}_{7-x}$ single crystals. Fitted coefficients are given in Table I. We have removed a large portion of the experimental data in order to show the trace of the theoretical curve more clearly.

III. DISCUSSION

The details of the experimental technique are presented in an earlier publication² in which we also describe the effects of a magnetic field on the thermal conductivity. Sample 1 and sample 2 correspond to identically designated samples in Ref. 2. Sample 1A is sample 1 after a large strain has been applied to it. (Sample 1 actually broke in a large magnetic field, while rotating the field. Fortunately, the break was at the base of the sample, and we were able to remount it, labeling it sample 1A.)

For $T > T_c$ the fit reflects the slow decrease in κ due to the increase in phonon-phonon Umklapp scattering as the temperature is raised. The curve, however, lies slightly below the data for $T > \sim 170$ K and for $T_c < T < \sim 125$ K. This deviation can be explained in the following way. For $T > \sim 170$ we expect the data to differ from the true value of the thermal conductivity due to radiation effects. By wrapping a resistive wire around the sample radiation shield, we were able to vary the temperature difference between the sample and the sample surroundings. In so doing we found that, in our experimental configuration, radiation effects become noticeable near 170 K and lead to about 10% error in κ at 200 K. This process is reflected in Fig. 1, where the data, uncorrected for radiation loss, lie artificially high due to the radiation contribution above ~ 170 K.

In the range $T_c < T < 125$ K we are assuming in our model that the electrical resistivity varies linearly with temperature. A closer analysis of resistivity measurements, however, indicates that for $T < \sim 120$ –150 K, the resistivity lies somewhat lower than a linear extrapolation from higher temperature values.¹⁴ This is attributed to superconducting fluctuations in which a small fraction of the electrons condense into Cooper pairs even above T_c . Although this process will act to decrease the electronic contribution to the thermal conductivity, the large increase in κ below T_c attests to the fact that the removal of conduction electrons from the system leads to an increase in the total thermal conductivity. This is due to an increase in the phonon mean-free path, and hence an increase in the lattice thermal conductivity. By ignoring fluctuation effects in our model we can then expect the theoretical curve to underestimate the data in this range.

Below T_c , the model describes the data extremely well. As the sample enters the superconducting domain, two competing contributions determine the slope of the increase in κ . The electronic contribution will fall steeply as the temperature is lowered below T_c , while the lattice contribution will increase rapidly. To successfully fit the data, there is a window of values that the coefficients which affect the shape of the theoretical curve in this temperature range, K , E , and χ , may have. A large K , corresponding to a large electronic contribution, κ_e , lowers the slope of the increase in κ below T_c . We find that a significant electronic contribution is required to fit the data, for example, $K = 4.4 \pm 1.1$ W/m K for sample 1, or $\sim 30\%$ of the total thermal conductivity. Invoking the Wiedemann-Franz law, this implies an electrical resistivity $\rho = 60 \pm 20 \mu\Omega$ cm, which is consistent with the directly measured value of ρ for similar specimens.

The theoretical curve is very sensitive to the scaled energy gap coefficient χ . With a larger gap, the electrons condense more rapidly with decreasing temperature. As indicated in Fig. 2(a) this leads to a steeper increase in κ_p , a wider hump below T_c , and a shift in the peak to higher temperature. We place bounds on the value of χ to satisfactorily fit our data at $\chi = 1.6 \pm 0.3$. The magnitude and nature of the superconducting energy gap is at present a subject of great interest. For instance, Kresin and Wolf¹⁵ propose that there are two distinct energy gaps in $\text{YBa}_2\text{Cu}_3\text{O}_{7-\delta}$ caused by the presence of overlapping energy bands. They cite a number of investigations, which have demonstrated the presence of two gaps. For example, Knight-shift studies indicate¹⁶ superconducting energy gaps associated with the chains and planes of the order $2\Delta_{ch}/k_B T_c = 3.5 (\chi = 1)$ and $2\Delta_{pl}/k_B T_c = 5 \pm 1 (\chi = 1.4 \pm 0.3)$, respectively. Anlage *et al.*,¹⁷ using a microstrip resonator technique, find that their data is well described by a single energy gap for $T > T_c/2$ with a value of $2\Delta/k_B T_c = 4.5 \pm 0.25 (\chi = 1.3 \pm 0.07)$. In the context of Ref. 14 this large gap value would be associated with the Cu-O planes. Similarly, our study, where the theoretical curve is sensitive to the value of χ for $T > \sim T_c/2$ [see Fig. 2(a)], indicates that the phonons re-

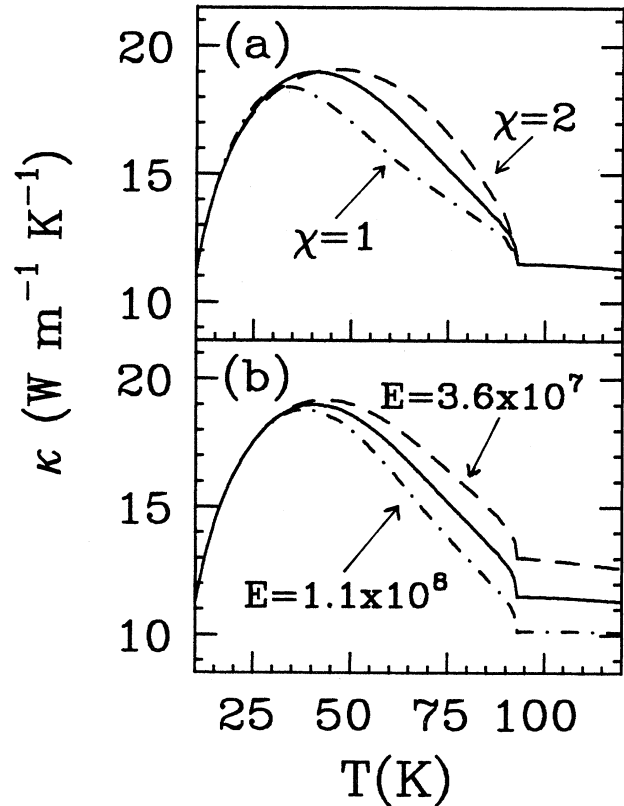


FIG. 2. Theoretical fits for sample 2 illustrating the dependence of κ on the values of the coefficients: (a) χ and (b) E . The solid line is determined by the coefficients in Table I, while the dashed and dot-dashed lines are obtained by varying the coefficients as indicated in the figures.

sponsible for in-plane heat transport couple most effectively to electrons whose superconducting gap energy is approximately $2\Delta/k_B T_c = 5.6 \pm 1.1$.

Our fit suggests that phonon-electron scattering, as reflected in the term $ETxg(x,y)$, is large for $T > T_c$ and then falls off rapidly for $T < T_c$ as the carriers condense into Cooper pairs until the contribution is negligible near $T_c/2$. The magnitude of E thus determines the relative increase of the thermal conductivity below T_c as compared to the value at T_c [see Fig. 2(b)]. E is directly proportional to the electron-phonon coupling constant λ , and ideally one can extract λ from a theoretical fit of this type. Tewordt and Wölckhausen⁷ derive the following equation to relate E and λ (adjusted for the different normalization of the phonon-electron scattering rate coefficient used in this study):

$$\lambda = \frac{2}{\pi} t \frac{a}{v} E, \quad (5)$$

where a is the unit cell length, t is the effective hopping matrix element for a two-dimensional tight-binding band of electrons, and v is the phonon velocity. Obtaining λ from E in this manner is complicated by the fact that there is more than one combination of parameters that yields an acceptable fit of the data, and, as a result, each coefficient has a range of possible values. For sample 1A, we find that E can vary from $1.3 \times 10^8 \text{ K}^{-1} \text{ sec}^{-1}$ to $3.1 \times 10^8 \text{ K}^{-1} \text{ sec}^{-1}$. Using $a = 4 \text{ \AA}$, $v = 5000 \text{ m/sec}$,¹⁸ and $t = 5000 \text{ K}$ in Eq. (5), this corresponds to a coupling strength in the range $0.03 < \lambda < 0.08$.

Values of $\lambda \sim 0.5$ and 0.6 have been reported by Tewordt and Wölckhausen⁷ for sintered $\text{YBa}_2\text{Cu}_3\text{O}_{7.8}$ and by Morelli *et al.*⁵ for single-crystal $\text{La}_{2-x}\text{Sr}_x\text{CuO}_x$, respectively. These values are clearly much larger than the value that we report for single-crystal $\text{YBa}_2\text{Cu}_3\text{O}_{7.8}$. We have, however, reevaluated the data used in the above-mentioned investigations and arrive at significantly lower values. For sintered $\text{YBa}_2\text{Cu}_3\text{O}_{7.8}$ (the data of Uher and Kaiser,¹⁹ also fit in Ref. 7), we find $0.04 < \lambda < 0.34$. This range is found by setting the coefficient for the electronic thermal conductivity κ_e , and the Umklapp scattering term U to zero (corresponding to the situation of Ref. 7) and allowing all other coefficients to vary until a curve, which describes the data qualitatively as well as that reported in Ref. 7 is achieved. In Ref. 7, the value of the boundary scattering limited mean free path L_b at which the authors arrive is an order of magnitude smaller than they expect. To accommodate this, they decrease the coefficient in the equation of the lattice thermal conductivity, Eq. (2), by a factor of 10 to obtain a different value for the boundary-scattering term, which corresponds to their desired L_b . Such a modification, in turn, increases the value they derive for λ by a factor of 10. We note, however, that, as described below for the single-crystal data, we find that the coefficient B for the ceramic data has a large range of acceptable values. We also note that there is a broad distribution of crystallite sizes, which will lead to uncertainty in the extraction of the boundary-scattering-limited mean free path. Because of these other possible sources of error in L_b , we do not believe that a

modification of Eq. (2), such as made in Ref. 7, is necessary, and we do not modify it in our analysis. For the $\text{La}_{2-x}\text{Sr}_x\text{CuO}_x$ single-crystal data of Ref. 5, we find $0.004 < \lambda < 0.01$, also much smaller than the value originally reported.²⁰

Reanalysis of the sintered $\text{YBa}_2\text{Cu}_3\text{O}_{7.8}$ and single-crystal $\text{La}_{2-x}\text{Sr}_x\text{CuO}_x$ data thus leads to values of the electron-phonon coupling strength that are much smaller than originally reported, and these values are consistent with the coupling strength we calculate for single-crystal $\text{YBa}_2\text{Cu}_3\text{O}_{7.8}$. We stress that this value, $0.03 < \lambda < 0.08$, is associated with the phonons responsible for the heat transport, i.e., with longitudinal-acoustic phonons of long wavelength, as will be shown below. We also note that the magnitude of λ is dependent on the applicability of Eq. (5).

One of the goals of this study is to determine which types of scatterers are most prominent in our crystals. By observing the form of the thermal resistance with a given scattering center removed, we are able to examine the relative importance of the various scattering mechanisms in different regions of the temperature range. Such a process is indicated in Fig. 3. Here the total lattice thermal resistance of sample 1A, fit with the coefficients given in Table I, is shown by a solid line. We then illustrate what the lattice thermal resistance would be if various phonon scattering centers were totally removed, thus indicating their relative contribution to the total lattice

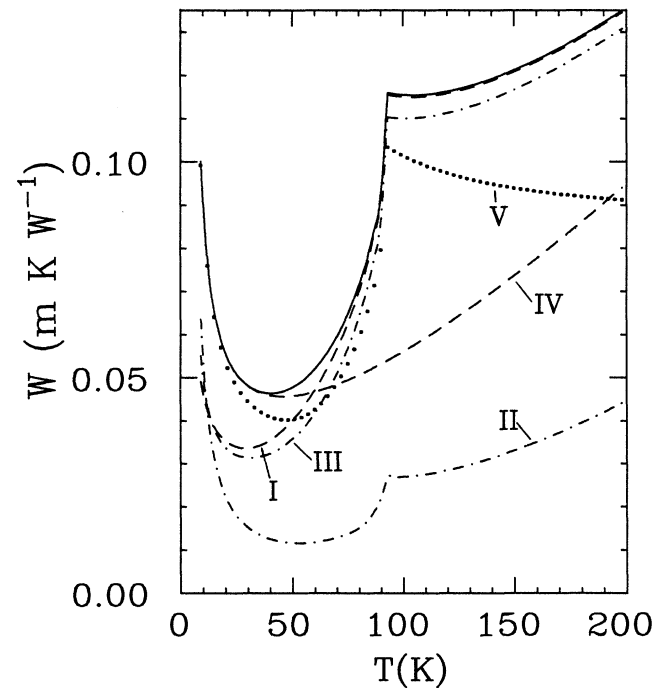


FIG. 3. Lattice thermal resistance (solid line) of sample 1A. The numbered curves indicate the lattice thermal resistance resulting when the following individual phonon-scattering terms, removed: I boundaries, II point defects, III sheetlike faults, IV electrons, and V other phonons (Umklapp scattering).

thermal resistance. In this manner we find that (1) point defects are a dominant phonon scatterer in the entire temperature range; (2) electrons are a major phonon scatterer, second only to point defects above T_c , and influence the flow of phonons at temperatures as low as 40K; and (3) boundary scattering is significant up to $T \sim 75$ K. We note that we did not find it necessary to include a tunnelling-state²¹ scattering term in order to obtain a good fit in the temperature range investigated.

For $T < \sim T_c/2$, phonons are scattered predominantly by the crystal boundaries and lattice defects. Hence the coefficients B , D_p , and D_{sf} determine the shape of the theoretical curve in this temperature range. These coefficients are determined by the microstructure of the sample, and thus their magnitudes provide insight into the degree of perfection of the crystal. For boundary scattering¹⁰

$$B = \frac{v}{L}, \quad (6)$$

where L is the smallest dimension of the crystal. We are able to obtain excellent fits to the data using values of B that correspond to the thicknesses of the various samples. It should be noted that of all the adjustable parameters B has, for a given sample, the widest range of acceptable values. This suggests that a large crystal with a greater concentration of defects can yield a thermal conductivity curve nearly identical to that of our smaller crystal with less defects.

The existence of significant boundary scattering for $T > 10$ K may, at first glance, seem surprising. A quick calculation of the phonon mean free path (MFP) l using the kinetic equation for the thermal conductivity of a gas to describe the lattice thermal conductivity,

$$\kappa_p = \frac{1}{3}c_v l v, \quad (7)$$

and using specific heat data of other investigators²² yields $0.007 \mu\text{m} < l < 1 \mu\text{m}$ for $10 \text{ K} < T < T_c$. This value of l is orders of magnitude less than the crystal width, and hence one might naively assume that κ should be unaffected by the boundaries of our crystal. This discrepancy can be explained as follows. As Fig. 3 indicates, point defects are the major source of scattering in our single-crystal specimens. Because the frequency dependence of the MFP for scatterers of this type is very strong, $l^{-1} \propto \omega^4$, phonons of high frequency are disproportionately affected, leaving a large part of the heat conduction to long-wavelength phonons with larger mean free paths. By evaluating the integrand of Eq. (2), the wavelength of the phonons that dominate the heat transport process can be calculated, and we find at 77 K a value of $\sim 100 \text{ \AA}$. The MFP of these phonons is $\sim 5 \mu\text{m}$, in contrast to the value of $0.01 \mu\text{m}$, which one derives from Eq. (7) at this temperature. In addition, phonons with MFP's as large as $50 \mu\text{m}$ make a non-negligible contribution to the integral. The "average" mean free path derived from Eq. (7), then, does not reflect the importance of long mean-free path phonons. A thorough discussion of this phenomenon was presented by Savvides and Goldsmid²³ in a study of the thermal conductivity of

irradiated silicon.

Ideally, one can extract the concentration of point defects and sheetlike faults from the values of the coefficients D_p and D_{sf} , respectively. However, the application of theoretical models predicting the magnitude of κ as a function of the concentration of defects is normally fraught with difficulties and estimates of this kind are typically not reliable.¹⁰ It is, however, interesting to look at the changes in D_p and D_{sf} from crystal to crystal, since these coefficients are proportional to the point defect and sheetlike fault densities.¹⁰ As discussed above, sample 1A is sample 1 after a large strain has been applied to it. Given the planar nature of the single crystals, we expect that a large strain will introduce sheetlike faults throughout the crystal. The theoretical fits of the data for samples 1 and 1A support this proposition. To successfully fit the data for sample 1A, all the coefficients from sample 1 can be retained except for the term that describes the scattering of phonons by sheetlike faults (Table I). Only by increasing the coefficient D_{sf} can we decrease the thermal conductivity by the appropriate amount throughout the entire temperature range. Note in the figure that the shift of the maximum value of κ in the data to a higher temperature is also perfectly matched by the adjustment of D_{sf} . Such consistency between the theoretical fit and the microstructure of the crystal provides further confirmation of the applicability of the model.

We see the same sort of consistency in the parameter D_p , which characterizes point-defect scattering. Sample 2 is a specimen with an oxygen content of $\delta = 0.16$, slightly higher than the value of sample 1, where $\delta = 0.1$. We thus expect greater point-defect scattering in sample 2. This is evident in both the generally lower thermal conductivity of sample 2 and the value of the coefficient D_p , which is larger for sample 2. Of course other defects, for example disorder in the cation layers and missing atoms from atomic sites other than the oxygen sites, will also contribute to phonon-point-defect scattering.

IV. CONCLUSION

In summary, we have described the thermal conductivity of single-crystal $\text{YBa}_2\text{Cu}_3\text{O}_{7.8}$ exceptionally well with a theoretical expression based on the model introduced by Tewordt and Wölkhausen. Small deviations between the data and the theoretical curve are attributed to superconducting fluctuations and radiation losses. We show the relative importance of the different scattering processes [boundaries, point defects, sheetlike faults, electrons, and other phonons (Umklapp scattering)] in the temperature range $10 \text{ K} < T < 180 \text{ K}$. Perhaps surprisingly, we show that the thermal transport is dominated by long-wavelength phonons and that phonon-boundary scattering is significant up to $T \sim 75$ K. The phonon-electron coupling strength for these phonons is calculated to lie in the range $0.03 < \lambda < 0.08$, and we believe the previous estimates of λ derived from thermal conductivity studies are an order of magnitude too large. In the context of an s -wave pairing mechanism, we find a significant electronic contribution to the thermal conductivity

(~ 4.4 W/mK or about 30% of the total thermal conductivity at T_c) and find that the dominant electron scatterers are phonons. Finally, we arrive at a value for the superconducting energy gap of $(1.6 \pm 0.3)\Delta_{\text{BCS}}(T)$.

ACKNOWLEDGMENTS

We thank Dr. Joshua Cohn and Dr. Donald Morelli for useful discussions during the course of this work and

Dr. Cohn for making available his fitting subroutine. We are grateful for the efforts of T. A. Vanderah in preparing the single crystals of $\text{YBa}_2\text{Cu}_3\text{O}_{7.8}$ for this research. This work was supported by the U.S. Army Research Office Contract No. DAAL-03-87-K-0007 and by a Grant from the Kellogg Foundation. F. N. acknowledges partial support from NSF Grant Nos. PHY89-04035 and DMR90-01502.

-
- ¹See, e.g., a review by C. Uher, *J. Supercond.* **3**, 337 (1990), and references therein.
- ²S. D. Peacor, J. L. Cohn, and C. Uher, *Phys. Rev. B* **43**, 8721 (1991).
- ³V. Florentiev, A. Inyushkin, A. Taldenkov, O. Melnikov, and A. Bykov, in *Progress in High Temperature Superconductivity*, edited by R. Nicolsky (World Scientific, Singapore, 1990), Vol. 25, p. 462.
- ⁴S. J. Hagen, Z. Z. Wang, and N. P. Ong, *Phys. Rev. B* **40**, 9389 (1989).
- ⁵D. T. Moreli, G. L. Doll, J. Heremans, M. S. Dresselhaus, A. Cassanho, D. R. Gabbe, and H. P. Jenssen, *Phys. Rev. B* **41**, 2520 (1990).
- ⁶M. F. Crommie and A. Zettl, *Phys. Rev. B* **43**, 408 (1991).
- ⁷L. Tewordt and Th. Wölkhausen, *Solid State Commun.* **70**, 839 (1989).
- ⁸L. Tewordt and Th. Wölkhausen, *Solid State Commun.* **75**, 515 (1990).
- ⁹J. Bardeen, G. Rickayzen, and L. Tewordt, *Phys. Rev.* **113**, 982 (1959).
- ¹⁰R. Berman, *Thermal Conduction in Solids* (University Press, Oxford, 1976).
- ¹¹B. T. Geilikman and V. Z. Kresin, *Kinetic and Non-Steady-State Superconductors* (Wiley, New York, 1974).
- ¹²L. Tewordt, *Phys. Rev.* **129**, 657 (1963).
- ¹³B. T. Geilikman, M. I. Duchanat, and V. R. Chechetkin, *Zh. Eksp. Teor. Fiz.* **73**, 2319 (1977) [*Sov. Phys. JETP* **46**, 1213 (1977)].
- ¹⁴U. Welp, S. Fleshler, W. K. Kwok, J. Downey, Y. Fang, and G. W. Crabtree, *Phys. Rev. B* **42**, 10 189 (1990); S. J. Hagen, Z. Z. Wang, and N. P. Ong, *ibid.* **38**, 7137 (1988); P. P. Freitas, C. C. Tsuei, and T. S. Plaskett, *ibid.* **36**, 833 (1987).
- ¹⁵V. Z. Kresin and S. A. Wolf, *Physica C* **169**, 476 (1990).
- ¹⁶S. E. Barrett, D. J. Durand, C. H. Pennington, C. P. Slichter, T. A. Friedmann, J. P. Rice, and D. M. Ginsberg, *Phys. Rev. B* **41**, 6283 (1990).
- ¹⁷S. M. Anlage, B. W. Langley, G. Deutschler, J. Halbritter, and M. R. Beasley (unpublished).
- ¹⁸P. B. Allen, in *Physical Properties of High Temperature Superconductors I*, edited by D. M. Ginsberg (World Scientific, Singapore, 1989), Chap. 5.
- ¹⁹C. Uher and A. B. Kaiser, *Phys. Rev. B* **36**, 5680 (1987).
- ²⁰Private communication with the authors of Ref. 5 confirms that the value originally reported deviates from ours by a factor of 100 due to an error in their original calculation.
- ²¹M. Nunez Regueiro, P. Esquinazi, M. A. Izbinsky, D. Esparza, and C. D'Ovidio, *Phys. Rev. B* **36**, 8813 (1987).
- ²²A. Junod, in *Physical Properties of High Temperature Superconductors II*, edited by D. M. Ginsberg (World Scientific, Singapore, 1990), Chap. 2.
- ²³N. Savvides and H. J. Goldsmid, *Phys. Lett.* **41A**, 193 (1972); *Phys. Status Solidi B* **63**, K89 (1974).